J. Fluid Mech. (2008), *vol.* 617, *pp.* 301–326.
doi:10.1017/S0022112008004278 Printed in the United Kingdom

Stability analysis of stratified shear flows with a monotonic velocity profile without inflection points. Part 2. Continuous density variation

S. M. CHURILOV†

Institute of Solar–Terrestrial Physics (ISTP), Siberian Department of Russian Academy of Sciences, Irkutsk 33, PO Box 291, 664033, Russia

(Received 25 December 2006 and in revised form 4 September 2008)

We investigate stability with respect to two-dimensional (independent of z) disturbances of plane-parallel shear flows with a velocity profile $V_x = u(y)$ of a rather general form, monotonically growing upwards from zero at the bottom ($y = 0$) to U_0 as $y \to \infty$ and having no inflection points, in an ideal incompressible fluid stably stratified in density in a layer of thickness ℓ, small as compared to the scale L of velocity variation. In terms of the 'wavenumber k – bulk Richardson number J' variables, the upper and lower (in J) boundaries of instability domains are found for each oscillation mode. It is shown that the total instability domain has a lower boundary which is convex downwards and is separated from the abscissa (k) axis by a strip of stability $0 < J < J_0^{(-)}(k)$ with minimum width $J_* = O(\ell^2/L^2)$ at $kL = O(1)$. In other words, the instability domain configuration is such that three-dimensional (oblique) disturbances are first to lose their stability when the density difference across the layer increases. Hence, in the class of flows under consideration, it is a three- not two-dimensional turbulence that develops as a result of primary instability.

1. Introduction

Vertical density stratification plays an important role in the dynamics of geophysical flows; in particular, it usually has a determining influence on their stability. On the other hand, stratification combined with velocity shear makes theoretical analysis of stability an extremely difficult problem. In such a situation, of particular interest are those special properties of flows that simplify the task of a researcher. For instance, in high-Prandtl-number media (for example, in sea water) changes in density occur, as a rule, sharply, in thin transitional layers outside of which the density is almost constant (e.g. Turner 1973). Owing to this, characteristic scales of velocity (L) and density (ℓ) variations in flows of such media appear to be essentially different, $\ell \ll L$, and this fact is actually equivalent to separation in space of the effects of stratification and velocity shear. In a narrow layer where stratification is strong, the velocity shear can be treated as a correction, and at the same time outside of this layer the flow may be considered as approximately homogeneous, taking stratification into account as a small perturbation.

† Email address for correspondence: churilov@iszf.irk.ru

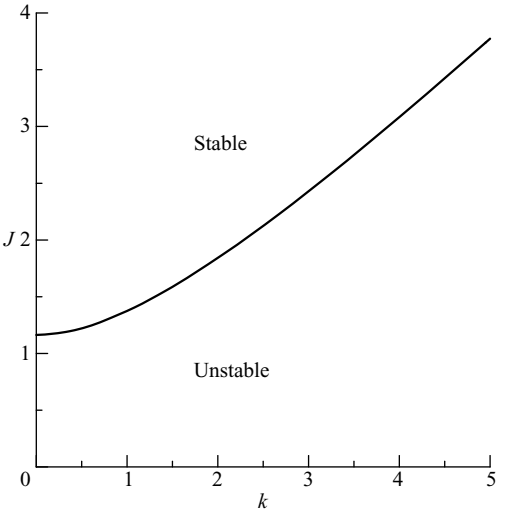

FIGURE 1. Stability diagram for a two-layer flow ($\ell = 0$; $u(y) = 1 - e^{-y}$, $y_N = 0.5$).

Churilov (2004, 2005), proposed a method of investigation of such flows at high Reynolds numbers based on a semi-qualitative solution of the Taylor–Goldstein equation using well-known properties of solutions of the Rayleigh equation. In the context of the method, a conclusion about flow stability (or instability) is dictated by the presence or absence of some fairly general features of the flow and consequently holds true for a wide enough class of flows. First of all, the method was used for stability analysis of flows with inflection-free velocity profiles because the properties of solutions of the Rayleigh equation are simplest in this case.

Such flows are stable in a homogeneous medium (according to Rayleigh's theorem, see, for example, Turner 1973; Dikii 1976; Drazin & Reid 1981), but may lose their stability in stratified media. Chimonas (1974) appears to be the first to argue thoroughly for this possibility, and the instability itself was found numerically by Fua, Einaudi & Lalas (1976) for an atmospheric boundary-layer flow with $\ell = O(L)$. The stability of flows belonging to this class was also studied later (see, for example, Redekopp 2001).

Churilov (2004, 2005) considered a similar problem in the limit $\ell \to 0$, i.e. in a two-layer medium with density $\rho(y) = \{\rho_1,\ 0 \leqslant y < y_N;\ \rho_2,\ y_N < y < \infty\}$ where $\rho_2 < \rho_1$. He studied the stability of plane-parallel flows in the gravity field g, with an arbitrary inflection–free velocity profile $v_x = u(y)$ that monotonically increases upwards from zero at the bottom ($y = 0$) to some finite value U_0 as $y \to \infty$. It was found that such flows lose stability at an arbitrarily small density difference and remain unstable for any $\rho_1/\rho_2 > 1$. Moreover, in the general case (when $u'' \equiv \mathrm{d}^2u/\mathrm{d}y^2 < 0$ everywhere) the instability domain configuration on the 'dimensionless wavenumber kL – the bulk Richardson number $J = (gL/U_0^2)\ln(\rho_1/\rho_2)$' plane appears to be universal (see figure 1). (Hereinafter, we shall use dimensionless variables scaled by L, U_0 and ρ_1.) Dispersion curve $J = J_1(k)$ of waves propagating with limiting velocity of the flow ($c = 1$) separates stable and unstable perturbation domains: the region of neutrally stable oscillations overtaking the flow ($c > 1$) is located above it, whereas the strip $0 < J < J_1(k)$ is filled by unstable oscillations with $c_r \equiv \mathrm{Re}\, c$ increasing from $u_N \equiv u(y_N)$ at $J = 0$ to 1 at $J = J_1(k)$.

When $\ell = 0$, the role of stratification is minimal: it appears only in the condition of matching the solutions of the Rayleigh equation at the interface. For this reason, many interesting and important features due to stratification remain beyond our scope and, when applied to real flows, the results of such a stability analysis should be considered as a first approximation. The objective of this paper is to investigate the stability of the same class of flows in the case where the density decreases continuously and monotonically from ρ_1 to ρ_2 in a transitional layer of small, but finite, thickness ℓ which is centred at $y = y_N$. Let us try to conceive what spectrum should be expected in this case.

As stratification is strongly localized, in the bulk of the flow (where $|y - y_N| \gg \ell$) disturbances obey, in fact, the Rayleigh equation. In this case, there are no waves running to infinity in y, and the flow can be regarded as a waveguide, and its eigenoscillations as guided waves, with sinusoidal horizontal and modal vertical structure. When $u''(y) \neq 0$ everywhere, solutions of the Rayleigh equation are known to have no more than one zero (see, for example, Dikii 1976; Drazin & Reid 1981), and this zero is at the bottom ($y = 0$) in the lower (nearly) homogeneous layer or at the infinity in the upper one. That is why, at $\ell = 0$, eigenoscillations have no nodes in y.

When $0 < \ell \ll 1$, the waveguide also has nodeless eigenoscillations. In addition, there should be eigenmodes with nodes in y as well, but all these nodes must be located inside the stratified (transitional) layer. We shall show that for $\ell \neq 0$, the physical nature of stability boundaries remains the same as it is at $\ell = 0$. Recall that, according to Howard's (1961) semicircle theorem (see also Turner 1973; Dikii 1976; Drazin & Reid 1981; Timofeev 2000), each unstable perturbation is in phase resonance with the flow at a critical level $y = y_c$ determined by the condition that the real part of the phase velocity, c_r, coincides with the flow velocity, $c_r = u(y_c)$. As J increases, c_r grows, the critical level is gradually displaced toward the flow periphery and disappears when $c \geqslant 1$ because the perturbation is no longer in resonance with the flow. Hence, the dispersion curve $J = J_m(k; 1)$ of neutral oscillations belonging to the mth mode and having phase velocity $c = 1$ is the upper boundary of the corresponding instability domain. On the other hand, as J decreases, the critical level moves towards the region of strong stratification, and when it 'intrudes' into this region the oscillation becomes stable at some $J = J_m^{(-)}(k) > 0$. This is the lower boundary of the mth instability domain.

Thus, when $\ell \neq 0$ there should be a denumerable set of eigenmodes (numerated by m) with similar spectra (stability diagrams). The stability diagram of the nodeless ($m = 0$) mode should be almost the same as for $\ell = 0$ (see figure 1), differing only by the stability strip $0 < J < J_m^{(-)}(k)$ in the lower part. The other diagrams (with $m > 0$) can be made from it, roughly speaking, by stretching m^2/ℓ times in J. For example, let us consider eigenoscillations with $c = 1$ (lying on the upper boundaries of instability domains). When $m = 0$, they obey the dispersion relation $J = J_0(k; 1) \approx J_1(k) = O(1)$. If, however, the eigenfunction has m nodes (located inside the transitional layer), it can be easily seen from the Taylor–Goldstein equation, (2.3) below, that

$$\frac{J_m(k;1)\, n(y)}{(1-u_N)^2}\, \ell^2 = O(m^2) \quad \text{or} \quad J_m(k;1) = O(m^2/\ell),$$

where $u_N = u(y_N)$ (note that $n(y) = O(\ell^{-1})$, see (2.1)).

We shall see that this rough reasoning is quite realistic and can be supported by mathematically consistent consideration of the problem. However, a part of this

consideration, namely, calculating the lower boundaries $J = J_m^{(-)}(k)$ of instability domains, requires a rather complicated and refined analysis. For this reason, the paper is organized as follows. The mathematical statement of the problem, as well as model velocity and density profiles used for illustrative calculations (equation (2.5)), are given in § 2. In the following two sections we outline all the key points, formulae and results of the stability analysis leaving detailed mathematics for the Appendices (available as a supplement to the online version of the paper). And in § 5 the basic results are formulated and discussed.

2. Statement of the problem

We consider a steady-state plane-parallel flow of ideal stably stratified incompressible fluid in the half-space $y \geqslant 0$. Its velocity grows monotonically from zero at $y = 0$ to 1 as $y \to \infty$, so that (the prime denotes the derivative in y)

$$u(0) = 0, \quad u'(0) = 1, \quad \lim_{y\to\infty} u(y) = 1; \quad u'(y) > 0, \quad u''(y) < 0.$$

In the Boussinesq approximation, the stratification appears in equations via the squared Brunt–Väisälä frequency which can be written in the form

$$\Omega^2(y) \equiv -\frac{g}{\rho}\frac{\mathrm{d}\rho}{\mathrm{d}y} = J\,n(y), \quad n(y) = \frac{\mathrm{d}}{\mathrm{d}y}\left(\frac{\ln\rho}{\ln\rho_2}\right) \geqslant 0,$$

where J is the previously introduced bulk Richardson number and, obviously,

$$\int_0^\infty \mathrm{d}y\, n(y) = 1. \tag{2.1}$$

We assume that the function $n(y)$ is localized in a layer of thickness $\ell \ll 1$ with the centre at

$$y_N = \int_0^\infty \mathrm{d}y\, y\, n(y), \tag{2.2}$$

has a single maximum, and rapidly (at least, exponentially) tends to zero outside the layer. The layer is located in such a manner that the flow velocity inside it, u_N, is close to neither zero nor unity.

The spectral stability of the flow is investigated with respect to two-dimensional perturbations described in terms of the streamfunction ψ ($v_x = u(y) + \partial\psi/\partial y$, $v_y = -\partial\psi/\partial x$). In the linear approximation, $\psi = g(y)\exp(-\mathrm{i}\omega t + \mathrm{i}kx)$ satisfies the Taylor–Goldstein equation (see, for example, Turner 1973; Dikii 1976; Drazin & Reid 1981) with boundary conditions at $y = 0$ and $y \to \infty$:

$$\frac{\mathrm{d}^2 g}{\mathrm{d}y^2} + \left[\frac{J\,n(y)}{(u-c)^2} - \frac{u''}{u-c} - k^2\right] g = 0; \quad g(0) = 0, \quad |g(\infty)| < \infty. \tag{2.3}$$

The problem consists in finding the (generally complex) eigenvalues of the phase velocity,

$$\frac{\omega}{k} = c(k, J) \equiv c_r(k, J) + \mathrm{i}\,c_i(k, J),$$

and boundaries of the instability domain. (Any of the numbers J, k and c (at given values of two others) can be treated as an eigenvalue, but only c can take complex values, and in this case it is more convenient to search for c at given J and k.)

Since the stratification is strongly localized, it is convenient to divide the flow into the inner ($|y - y_N| = O(\ell)$) region containing the transitional layer with significant

changes in density, and the outer ($|y-y_N| \gg \ell$) regions with nearly constant densities, to solve (2.3) separately in these regions and then to match the solutions in domains $\ell \ll |y-y_N| \ll 1$, where they overlap, using the multiple scale method (see, for example, Nayfeh 1973). For this purpose, we introduce the inner variable Y and the function $N(Y) = \ell\, n(y)$ which satisfy the relations (compare with (2.1) and (2.2))

$$y - y_N = \ell Y; \quad \int_{-\infty}^{\infty} \mathrm{d}Y\, N(Y) = 1, \quad \int_{-\infty}^{\infty} \mathrm{d}Y\, Y\, N(Y) = 0, \tag{2.4}$$

(the last two are accurate to exponentially small terms because the lower limit in integrals is actually equal to $-y_N/\ell$).

The Taylor–Goldstein equation (2.3) has a singularity at the critical level $y = y_c$. For this reason, the presence (or absence) and position of the critical level are both very important for our problem, and its position with respect to the stratified (transitional) layer is the most essential. If there is no critical level or it is located outside of the transitional layer ($|y_c - y_N| \gg \ell$) the equation (2.3) has no singularity in the layer, and we have a rather simple regular inner problem (RIP) considered in § 3. Otherwise, we are confronted with a much more difficult singular inner problem (SIP) which will be analysed in § 4.

We shall illustrate our analysis using the results of calculations for a model flow

$$u(y) = 1 - \exp(-y), \quad n(y) = \frac{1}{\ell\sqrt{\pi}} \exp\left[-\frac{(y-y_N)^2}{\ell^2}\right], \tag{2.5}$$

with $\ell = 0.01$ and $y_N = 0.5$. The same calculations were also done for the flow

$$u(y) = \tanh(y), \quad n(y) = \left[2\ell \cosh^2\left(\frac{y-y_N}{\ell}\right)\right]^{-1},$$

and very similar results were obtained. (We use a fourth-order Runge–Kutta method for integrating differential equations, shooting when searching for eigenvalues, and Simpson's formula for integrals.)

3. Regular inner problem

3.1. *General consideration and 'fast'* ($c \geqslant 1$) *neutral waves*

First of all, we turn to oscillations overtaking the flow and hence having no critical level. At fixed $c \geqslant 1$ and $k \geqslant 0$, the problem (2.3) is a Schrödinger (or Sturm–Liouville) eigenvalue problem: the eigenvalues J should be found for which there is a level with 'energy' $E = -k^2$ in the potential well

$$V(y) = -\frac{J\, n(y)}{[c-u(y)]^2} - \frac{u''(y)}{c-u(y)},$$

bounded on the left (at $y = 0$) by a reflecting wall. The characteristic width of the well is equal to the thickness of the stratified layer ℓ, and its depth is proportional to J, therefore, the number of eigenvalues is not limited and, as would be expected, they form a denumerable set: $J = J_m(k; c)$, $m = 0, 1, 2, \ldots$. To have a more detailed picture, let us consider the outer and the inner problems separately and then match their solutions.

In outer regions, (2.3) reduces to the Rayleigh equation with exponentially small corrections for stratification. Its solutions above (g_+) and below (g_-) the transitional

layer (each obeying the proper boundary condition, see (2.3)) can be represented (as $y \to y_N$) in the form of series in ℓ (hereinafter, notations $f_N = f(y_N)$ and $f_c = f(y_c)$ are used):

$$g_\pm(y) = g_{\pm N} + g'_{\pm N}(y - y_N) + \cdots = g_{\pm N} + \ell g'_{\pm N} Y + O(\ell^2 Y^2), \tag{3.1}$$

where $(g'_N/g_N)_\pm$ depend on k and c.

Passing in (2.3) to the variable Y (see (2.4)) yields, up to terms of $O(\ell^2)$ inclusive,

$$\frac{\mathrm{d}^2 g}{\mathrm{d}Y^2} + \left\{ R\,N(Y)\left[1 + \frac{2\ell u'_N Y}{c - u_N} + \ell^2\left(\frac{u''_N}{c - u_N} + \frac{3u'^2_N}{(c - u_N)^2}\right)Y^2\right] + \ell^2\left(\frac{u''_N}{c - u_N} - k^2\right)\right\} g = 0, \tag{3.2}$$

where

$$R = \frac{\ell J}{(c - u_N)^2} \quad \text{or} \quad J = \ell^{-1} R\,(c - u_N)^2. \tag{3.3}$$

This is the equation of RIP, and the density stratification is of first importance in it, whereas the velocity shear is considered as a correction. The solution of (3.2) is sought in the form of expansion in ℓ,

$$g(Y) = g^{(0)}(Y) + \ell g^{(1)}(Y) + \ell^2 g^{(2)}(Y) + \cdots, \quad R = R^{(0)} + \ell R^{(1)} + \ell^2 R^{(2)} + \cdots. \tag{3.4}$$

To obtain the dispersion relation $c = c(k, J)$, we should calculate asymptotic expansions of the inner solution $g(Y)$ as $Y \to \pm\infty$ and match them to (3.1) when $1 \ll |Y| \ll \ell^{-1}$ for each order in ℓ.

If perturbations are not too short-wavelength ($k\ell \ll 1$), equation (3.2) at $O(1)$ is reduced to the problem (boundary conditions are due to the fact that at $O(1)$, $g_\pm(y) = g_{\pm N} = \text{const}$ in (3.1))

$$\frac{\mathrm{d}^2 g^{(0)}}{\mathrm{d}Y^2} + R^{(0)} N(Y)\, g^{(0)} = 0, \quad \lim_{Y \to \pm\infty} \frac{\mathrm{d}g^{(0)}}{\mathrm{d}Y} = 0 \tag{3.5}$$

of zero energy levels in a potential well $V_0(Y) = -R^{(0)} N(Y)$ (the existence of such levels is guaranteed by a fast enough tending of $N(Y)$ to zero as $Y \to \pm\infty$, see, for example Calogero 1967) the depth of which is regulated by the parameter $R^{(0)}$. Evidently, the problem (3.5) has a denumerable set of eigenvalues $R^{(0)}_m$. Note that $R^{(0)}_0 = 0$ for any $N(Y)$ so that $R_0 = \ell R^{(1)}_0 + \cdots = O(\ell)$, whereas the following ($m \geqslant 1$) eigenvalues $R^{(0)}_m$ are of $O(1)$ and grow with m as m^2. Dependence of R_m on k is weak enough and can be found in higher orders of the expansion (3.4). If, however, perturbations are very short-wavelength, $k\ell = O(1)$, we have in the main order a somewhat different spectral problem,

$$\frac{\mathrm{d}^2 g^{(0)}}{\mathrm{d}Y^2} + \left[R^{(0)} N(Y) - k^2\ell^2\right] g^{(0)} = 0, \quad \left|g^{(0)}(\pm\infty)\right| < \infty. \tag{3.6}$$

Its eigenvalues $R^{(0)}_m(k\ell)$ grow both with m and $k\ell$, and in the limit $k\ell \to 0$ become the eigenvalues of the problem (3.5).

With $N(Y) = (1/2)\,\mathrm{sech}^2 Y$, (3.6) can be reduced to the Gegenbauer equation (Abramowitz & Stegun 1964), and the spectrum can be found analytically:

$$R^{(0)}_m = 2(m + k\ell)(m + k\ell + 1) \xrightarrow{k\ell \ll 1} 2m(m + 1). \tag{3.7}$$

Note that eigenvalues with $m \geqslant 1$ can be also approximately calculated by WKB (or Liouville–Green, see, for example, Nayfeh 1973; Olver 1974) method which yields

$$R_m^{(0)} = \pi^2 \left(m + \tfrac{1}{2}\right)^2 \Big/ \left[\int_{-\infty}^{\infty} \mathrm{d}Y \sqrt{N(Y)}\right]^2 \tag{3.8}$$

for the problem (3.5), and a somewhat more complicated formula for the problem (3.6). In particular, using (3.8) we find that (compare with (3.7))

$$R_m^{(0)} = 2\left(m + \tfrac{1}{2}\right)^2 \quad \text{for} \quad N(Y) = \tfrac{1}{2}\,\mathrm{sech}^2 Y,$$

$$R_m^{(0)} = \frac{\pi^{3/2}}{2}\left(m + \tfrac{1}{2}\right)^2 \quad \text{for} \quad N(Y) = \frac{1}{\sqrt{\pi}}\,\mathrm{e}^{-Y^2}.$$

Eigenfunctions $g_m^{(0)}(Y) \equiv s_m(Y)$ of the problem (3.5) (m is the number of nodes) are conveniently normalized by $s_m(+\infty) = 1$ so that

$$s_m(+\infty) = 1, \quad s_m(-\infty) = (-1)^m a_m, \quad m = 0, 1, 2, \ldots . \tag{3.9}$$

Numbers $a_m > 0$ depend on the $N(Y)$ behaviour: if, for example, $N(Y)$ is even, all $a_m = 1$. Matching to $g_{\pm}(y)$ yields (see (3.1))

$$g_{+N} = 1, \quad g_{-N} = (-1)^m a_m + O(\ell).$$

The second (linearly independent) solution $h_m(Y)$ of (3.5) is specified by the condition

$$\lim_{Y \to +\infty} [h_m(Y) - Y] = 0 \quad \text{so that} \quad W(s_m,\, h_m) = s_m\, h_m' - s_m'\, h_m = 1$$

(the prime denotes a derivative in independent variable, i.e. in Y). As $Y \to -\infty$,

$$h_m(Y) = \frac{(-1)^m}{a_m}(Y + b_m) + \mathrm{EST}, \tag{3.10}$$

where b_m are some real numbers, and EST denotes hereinafter exponentially small terms which are due to the stratification rapidly decaying with $|Y|$.

The case $m = 0$ is special because

$$R_0^{(0)} = 0, \quad s_0(Y) \equiv 1, \quad h_0(Y) = Y,$$

for any $N(Y)$. In the next order, $O(\ell)$, (3.2) yields

$$\frac{\mathrm{d}^2 g_0^{(1)}}{\mathrm{d}Y^2} = -R_0^{(1)}\, N(Y), \quad g_0^{(1)} = -R_0^{(1)} \int_Y^{\infty} \mathrm{d}Y_1 (Y_1 - Y)\, N(Y_1) + \alpha\, Y.$$

As $Y \to +\infty$, $g_0^{(1)} = \alpha\, Y + \mathrm{EST}$, and when $Y \to -\infty$ using (2.4) we obtain

$$g_0^{(1)} = \left(\alpha + R_0^{(1)}\right) Y + \mathrm{EST}.$$

Matching it to (3.1) we see that $\alpha = g_{+N}'/g_{+N}$ and

$$R_0^{(1)} \equiv \frac{J_0^{(1)}}{(c - u_N)^2} = \left(\frac{g_-'}{g_-} - \frac{g_+'}{g_+}\right)_{y = y_N} = \frac{g_{-N}'}{g_{-N}} - \frac{g_{+N}'}{g_{+N}}. \tag{3.11}$$

This coincides exactly with the dispersion relation in two-layer ($\ell = 0$) flows (see Churilov 2004, 2005) whereas the parameter ℓ will appear only together with higher

terms of the expansion of R_0. In particular, at $O(\ell^2)$

$$\frac{\mathrm{d}^2 g_0^{(2)}}{\mathrm{d}Y^2} = -R_0^{(1)}\, N(Y)\, g_0^{(1)} - \left(R_0^{(2)} + \frac{2u'_N\, R_0^{(1)}}{c-u_N}\, Y \right) N(Y) - \frac{u''_N}{c-u_N} + k^2,$$

$$g_0^{(2)} = \left(k^2 - \frac{u''_N}{c-u_N} \right) \frac{Y^2}{2} - \int_Y^\infty \mathrm{d}Y_1\, (Y_1 - Y) \left[R_0^{(1)}\, g_0^{(1)}(Y_1) + R_0^{(2)} + \frac{2u'_N\, R_0^{(1)}}{c-u_N}\, Y_1 \right] N(Y_1).$$

Matching to (3.1) yields

$$R_0^{(2)} = -R_0^{(1)} \int_{-\infty}^\infty \mathrm{d}Y N(Y)\, g_0^{(1)}(Y) = R_0^{(1)^2} \int_{-\infty}^\infty \mathrm{d}Y N(Y) \int_Y^\infty \mathrm{d}Y_1 (Y_1 - Y)\, N(Y_1)$$
$$= 2\, R_0^{(1)^2} \int_{-\infty}^\infty \mathrm{d}Y N(Y) \int_Y^\infty \mathrm{d}Y_1 Y_1\, N(Y_1) = 2\, R_0^{(1)^2} \int_{-\infty}^\infty \mathrm{d}Y Y\, N(Y) \int_{-\infty}^Y \mathrm{d}Y_1 N(Y_1). \tag{3.12}$$

The integral on the right-hand side of (3.12) is positive and is easily calculated with model $N(Y)$ profiles

$$R_0^{(2)} = \frac{R_0^{(1)^2}}{2} \quad \text{for} \quad N(Y) = \tfrac{1}{2}\,\mathrm{sech}^2 Y, \qquad R_0^{(2)} = \frac{R_0^{(1)^2}}{\sqrt{2\pi}} \quad \text{for} \quad N(Y) = \frac{1}{\sqrt{\pi}}\, \mathrm{e}^{-Y^2}.$$

Thus, the more precise dispersion relation has the form

$$\frac{J_0}{(c-u_N)^2} = R_0^{(1)} + 2\ell R_0^{(1)^2} \int_{-\infty}^\infty \mathrm{d}Y N(Y) \int_Y^\infty \mathrm{d}Y_1 Y_1\, N(Y_1) + O(\ell^2). \tag{3.13}$$

Let us now turn to modes with $m \geqslant 1$. At $O(\ell)$, we obtain from (3.2) that

$$\frac{\mathrm{d}^2 g_m^{(1)}}{\mathrm{d}Y^2} + R_m^{(0)}\, N(Y)\, g_m^{(1)} = -\left(R_m^{(1)} + \frac{2u'_N\, R_m^{(0)}}{c-u_N}\, Y \right) N(Y)\, s_m(Y),$$

$$g_m^{(1)} = -\int_Y^\infty \mathrm{d}Y_1 \left(R_m^{(1)} + \frac{2u'_N R_m^{(0)}}{c-u_N} Y_1 \right) N(Y_1)\, s_m(Y_1) [s_m(Y)\, h_m(Y_1) - s_m(Y_1)\, h_m(Y)] + \beta\, h_m(Y),$$

matching to (3.1) yields

$$\left.\begin{aligned} I^{(m)} R_m^{(1)} &= a_m^2 \frac{g'_{-N}}{g_{-N}} - \frac{g'_{+N}}{g_{+N}} - \frac{2u'_N\, R_m^{(0)}}{c-u_N} \int_{-\infty}^\infty \mathrm{d}Y Y\, N(Y) s_m^2(Y), \\ I^{(m)} &= \int_{-\infty}^\infty \mathrm{d}Y N(Y)\, s_m^2(Y) > 0, \end{aligned}\right\} \tag{3.14}$$

and the dispersion relation has the form (compare with (3.13))

$$\frac{J_m}{(c-u_N)^2} = \ell^{-1} R_m = \ell^{-1} R_m^{(0)} + R_m^{(1)} + O(\ell). \tag{3.15}$$

If $N(Y)$ is even, (3.14) becomes simpler (compare with (3.11)):

$$R_m^{(1)} = \frac{1}{I^{(m)}} \left(\frac{g'_{-N}}{g_{-N}} - \frac{g'_{+N}}{g_{+N}} \right).$$

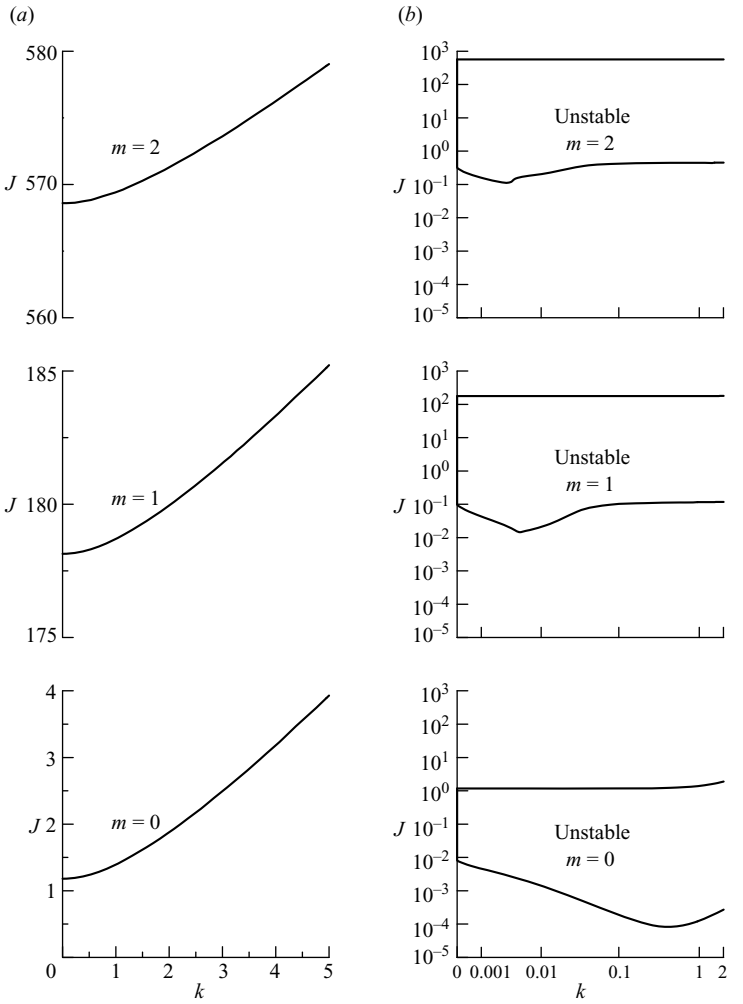

FIGURE 2. (*a*) Upper boundaries, and (*b*) configuration of particular instability domains.

In particular,

$$R_m^{(1)} = (2m+1)\left(\frac{g'_{-N}}{g_{-N}} - \frac{g'_{+N}}{g_{+N}}\right) \quad \text{when} \quad N(Y) = \tfrac{1}{2}\,\mathrm{sech}^2 Y.$$

Note, by the way, that if we put $m = 0$ in (3.14) (i.e. $a_0 = 1$, $s_0(Y) \equiv 1$, $R_0^{(0)} = 0$) we obtain the relation (3.11) so that we can use (3.14) for any m.

As $c \geqslant 1$, $g_{\pm}(y)$ are real and the dispersion relations (3.13) and (3.15) are also real, and they can be considered as expansions of J_m in ℓ under fixed c and k. Functions $J_m(k;c)$ increase monotonically both with k and c, and that is why the curve $J = J_m(k;1)$ serves as the lower boundary on the $(k,\ J)$-plane for the mth family of neutral modes overtaking the flow. Note that $J_0(k;1) = O(1)$ (when $k\ell \ll 1$) and tends to $J = J_1(k)$ (see figure 1) as $\ell \to 0$, whereas curves $J = J_m(k;1)$ with $m \geqslant 1$ lie much higher. Namely, each subsequent curve $J = J_{m+1}(k;1)$ is higher than the preceding (the mth) by $\Delta J = O(\ell^{-1}) \gg 1$ (see figure 2*a*), and when $\ell \to 0$ this step increases infinitely.

3.2. *Configuration of instability domains*

In the case of two-layer flows ($\ell = 0$) the domain of unstable oscillations lies immediately under the dispersion curve $J = J_1(k)$. Calculations yielding this result (see Appendix B, available as a supplement to the online version of the paper) are based on two circumstances, namely, on the existence of neutral oscillations with $c = 1$ and on the appearance of the critical level at the far periphery of the flow (where stratification is negligible; it is the assumption of fast (exponential) decrease of $n(y)$ as y recedes from y_N that is necessary for this) when $0 < 1 - c_r \ll 1$, and both of these are quite insensitive to distribution of density at $y = O(1)$, i.e. are valid for finite ℓ as well. Hence, for any k, the domain of unstable oscillations is necessarily adjacent to each dispersion curve $J = J_m(k;1)$ from below so that these curves serve simultaneously as the upper boundaries of particular instability domains.

In the absence of stratification (at $J = 0$), the flows under consideration are obviously stable, therefore, every mth domain of instability should have also a lower boundary, $J = J_m^{(-)}(k) > 0$. Approaching it from above, unstable oscillations (with $c_i > 0$) become stable ($c_i = 0$) and continue to be in phase resonance with the flow. Equation (2.3) in this case has a singularity at the critical level $y = y_c(k;m)$, and marginally stable oscillations have a spatial structure of singular neutral modes (Miles 1961, 1963). As long as the singularity is out of the transitional layer ($|y_c - y_N| \gg \ell$), the inner problem remains regular and the dispersion relations (3.13) and (3.15) are suitable for unstable and marginally stable oscillations as well. However, it is more convenient to treat them now as the equations for finding the complex phase velocity c for given J and k.

Note that in (3.15) the main term on the right-hand side is real, and only the next term, $R_m^{(1)}$, can be complex, therefore when $m \geqslant 1$, $c_i = \operatorname{Im} c = O(\ell)$ or it is less. On the contrary, the real and imaginary parts of the right-hand side of (3.13) are generally of the same order so that at $m = 0$, the order of magnitude of c_i is not related directly to ℓ and even $c_i = O(1)$ is possible. (Calculations made for some model velocity profiles (at $\ell = 0$) have demonstrated that $\max_{k,J} c_i \approx 0.07$, see Churilov 2005; Redekopp 2001.) However, our primary objective is to outline the boundaries of the instability domain, and therefore we assume that J and k are such that $|c_i| \ll |c_r - u_N|$, and we draw inferences about the stability of oscillations based on the sign of c_i. (It is well known that if the Taylor–Goldstein equation is regarded as a limit (at large Reynolds numbers) of the equations taking into account dissipation (viscosity, heat conduction, salt diffusion, etc.), then the limit for dissipative solutions is provided only by unstable ($c_i > 0$) and neutral ($c_i = 0$) solutions of (2.3) (in which the points of phase resonance are bypassed according to the Landau rule, see, for example, Dikii 1976; Timofeev 2000). On the contrary, its solutions with $c_i < 0$ (which formally implies damped oscillations) are not such a limit, and eigenoscillations of the flow corresponding to them probably do not exist.) In that case, the left-hand sides of the dispersion relations (3.13) and (3.15) can be written as

$$\frac{J_m}{(c-u_N)^2} \approx \frac{J_m}{(c_r-u_N)^2} - \frac{2\mathrm{i}J_m c_i}{(c_r-u_N)^3}, \quad m = 0,\ 1,\ 2, \ldots. \tag{3.16}$$

It is easy to see that the sign of c_i coincides with the sign of the imaginary part of R_m when $c_r < u_N$ and is opposite if $c_r > u_N$. To calculate R_m, it is necessary to know the outer solutions $g_{\pm}(y)$ when $\ell \ll |y - y_N| \ll 1$. Their behaviour essentially depends on k so we must consider the cases $k = O(1)$, $k \ll 1$ and $k \gg 1$ separately. These extensive calculations are given in Appendix A.

Summarizing their results, it is necessary to stress that eigenoscillations with a critical level outside of the transitional layer can be unstable or marginally stable if and only if their phase velocity is higher than the flow velocity in the transitional layer, $u_N < c_r \leqslant 1$ (remember that the same is true as $\ell = 0$). As for marginally stable oscillations of this class with $c_r < 1$, they exist only in the case of very long ($k < \ell \ll 1$) or short ($k \gg 1$) waves. In other words, RIP can describe the lower boundaries $J = J_m^{(-)}(k)$ of particular instability domains in the extremities of the spectrum leaving its middle band, $\ell < k \leqslant O(1)$, for SIP. The resulting configuration of instability domains (for the flow (2.5)) is shown in figure 2(*b*). Now we consider long- and short-wavelength bands in more detail.

3.2.1. *Long-wavelength band*

When $k \ll 1$ and $c_r > u_N$, we can show that (see Appendix A)

$$c_i = C_{m\,L}\left[k\,(1-c)^2 - J\int_{y_c}^{\infty} \mathrm{d}y_1\, n(y_1)\right] \quad (C_{m\,L} > 0). \tag{3.17}$$

The first term in square brackets 'provides' for instability (it is exactly the same as at $\ell = 0$) whereas the second term which is due to continuity of density variation (to 'spreading' of $n(y)$) is responsible for stabilization, and the boundary of the instability domain lies where

$$k\,(1-c)^2 = J\int_{y_c}^{\infty} \mathrm{d}y_1\, n(y_1). \tag{3.18}$$

Let us emphasize that the stabilizing effect is the stronger the smaller J is, therefore it is merely the lower boundary. It follows from (3.15) that (at given k) we can reduce J only by reducing $c - u_N$, i.e. making y_c closer to y_N, but in this case the integral of $n(y)$ increases very rapidly so that the right-hand side of (3.18) increases as well. (Also, this means that the marginally stable mode with $c < 1$ is unique for each m; and the same is true when $k \gg 1$, see (3.22).)

Relations (3.15) and (3.18) set $J_m^{(-)}(k)$ in a parametric form, $J = J_m(c)$ and $k = k_m(c)$. It is easily seen that J_m grows relatively slowly with increasing c whereas k decreases very rapidly. As $c \to 1$ (i.e. $y_c \to \infty$), $k \to 0$ and $J \to J_m(0;1)$, i.e. the upper and lower boundaries of the mth instability domain join at $k = 0$ (see figure 2*b*). To illustrate the lower boundary behaviour, we take (if $y - y_N \gg \ell$ only the asymptotic form of $n(y)$ is required)

$$n \approx n_0 \exp[-\beta(y - y_N)/\ell], \quad \beta = O(1). \tag{3.19}$$

Then

$$k\,(1-c)^2 = \frac{\ell J_m}{\beta}\, n_0 \exp[-\beta(y_c - y_N)/\ell] = \frac{R_m}{\beta}(c-u_N)^2 n_0 \exp[-\beta(y_c - y_N)/\ell], \tag{3.20}$$

and we see that the long-wavelength boundary of the instability domain is exponentially close to the ordinate axis (figure 2*b*) merging with it as $\ell \to 0$ (figure 1).

The inner problem remains regular as long as $|y_c - y_N| \gg \ell$. In the lower limit of this inequality, when $y_c - y_N \equiv \ell Y_c = O(\ell)$, we use (3.15) to obtain:

$$J_{m\geqslant 1}(c) \approx R_m\, {u'_N}^2\, \ell\, Y_c^2 = O(\ell), \quad \int_{y_c}^{\infty} \mathrm{d}y\, n(y) = O(1), \tag{3.21}$$

so that, according to (3.18), $k = O(\ell)$. Thus, we have described the lower boundaries $J = J_m^{(-)}(k)$ of particular instability domains when $0 \leqslant k < \ell$.

3.2.2. *Short-wavelength band*

When $k \gg 1$,

$$c_i = C_{m\,S}\left[\left(\frac{n_c'}{n_c} - 2k\right) Ri_c - \frac{u_c''}{u_c'}(1 + Ri_c)\right] \quad (C_{m\,S} > 0), \tag{3.22}$$

where $Ri(y) = Jn(y)/[u'(y)]^2$ is a local Richardson number. Here, the contributions due to stratification and velocity shear compete (recall that, $u_c'' < 0$, $n_c' < 0$ and $(-n_c'/n_c) = O(\ell^{-1}) \gg 1$), namely, velocity shear generates instability and stratification acts in a stabilizing manner and suppresses instability when

$$\frac{J}{{u_c'}^2}(n_c' - 2kn_c) = \left(1 + \frac{Jn_c}{{u_c'}^2}\right)\frac{u_c''}{u_c'} = \frac{u_c''}{u_c'}[1 + O(\ell)]. \tag{3.23}$$

Excluding the velocity c from (3.15) and (3.23), we obtain the equation $J = J_m^{(-)}(k)$ for the lower boundary of the mth instability domain in the short-wavelength region of the spectrum. For illustration, let us consider the same example (3.19) assuming $y_c - y_N \ll 1$. As $k \gg 1$, $g_{\pm}(y) \approx \exp(-k|y - y_N|)$ and (3.13)–(3.15) yield

$$J_m = \ell^{-1} R_m (c - u_N)^2 \approx \begin{cases} 2k{u_N'}^2 (y_c - y_N)^2, & m = 0, \\ \ell^{-1} R_m^{(0)} {u_N'}^2 (y_c - y_N)^2, & m \geqslant 1. \end{cases} \tag{3.24}$$

Substituting (3.19) into (3.23) and keeping in mind that $n_0 = O(\ell^{-1})$, we obtain the equation

$$Z^2 \mathrm{e}^{-Z} \approx -\frac{\ell\,\beta^2}{(\beta + 2k\ell)(n_0\ell)R_m}\frac{u_N''}{u_N'}, \quad Z = \beta(y_c - y_N)/\ell,$$

which implies that the difference

$$y_c - y_N \sim \ell \ln[(\beta + 2k\ell)R_m/\ell],$$

i.e. it is only logarithmically large compared with ℓ and exhibits a slow (logarithmic) growth with m and $k\ell$. Hence, $J_m^{(-)}(k)$ also slowly increases with k, mainly owing to increasing $R_m(k)$ (see figure 2*b*).

Thus, we have seen that $J_m^{(-)}(k)$ decrease with k when $k \ll 1$ and grow when $k \gg 1$, hence, they should take minimal values in the middle part of the spectrum where $u_N - c = O(\ell)$. If we note that $\min R_0^{(1)} = O(1)$ at $k = O(1)$ (see (3.11) and (4.5)) and use (3.15), we obtain an estimate

$$0 < \min_k J_0^{(-)}(k) = J_* = O(\ell^2), \quad 0 < \min_k J_{m\geqslant 1}^{(-)}(k) = O(\ell), \tag{3.25}$$

which will be supported by further analysis (see also figure 2*b*).

4. The singular inner problem

4.1. *Formulation of the problem*

If phase velocity of perturbation is such that $|c - u_N| = O(\ell)$, its critical level reaches the transitional layer, and the character of the inner problem changes dramatically so that it becomes singular (SIP). Passing to the inner variable Y in (2.3) while keeping in mind that $y_c - y_N = \ell Y_c = O(\ell)$ yields an equation up to terms of $O(\ell^2)$

inclusive ($P = J/\ell {u'_N}^2$)

$$\frac{\mathrm{d}^2 g}{\mathrm{d}Y^2} + \left\{ \frac{P\,N(Y)}{(Y-Y_c)^2}\left[1 - \frac{u''_N}{u'_N}\,\ell(Y+Y_c) + \frac{3u''^{\,2}_N}{4u'^{\,2}_N}\,\ell^2(Y+Y_c)^2 - \frac{u'''_N}{3u'_N}\,\ell^2\left(Y^2+Y_c^2+YY_c\right)\right] - \frac{\ell u''_N}{u'_N(Y-Y_c)}\left[1 - \frac{u''_N}{2u'_N}\,\ell(Y+Y_c) + \frac{u'''_N}{u''_N}\,\ell Y\right] - k^2\ell^2 \right\} g = 0, \qquad (4.1)$$

which has a singularity at $Y = Y_c$ (compare with (3.2)). We shall restrict our consideration to searching for marginally stable solutions for which $c_i = 0+$, and eigenfunctions are calculated by the Landau rule with bypassing of the singular point in the complex Y plane from below (see, for example, Dikii 1976; Drazin & Reid 1981; Timofeev 2000).

Equation (4.1) should be complemented by boundary conditions as $Y \to \pm\infty$ which can be found from matching to outer solutions $g_\pm(y)$ when $1 \ll |Y| \ll \ell^{-1}$. Furthermore, according to Miles (1961, 1963), the eigenfunction of marginally stable oscillation can be represented in the form (see also Drazin & Reid 1981)

$$g(Y) = (Y - Y_c)^\mu\, \tilde{g}(Y) \quad (0 \leqslant \mu \leqslant 1), \qquad (4.2)$$

where $\tilde{g}(Y)$ is an analytic function in the vicinity of Y_c. Substituting (4.2) into (4.1) we find easily that

$$\left.\begin{aligned} &\tfrac{1}{4} \geqslant \mu(1-\mu) = PN_c\left[1 - \frac{2u''_N}{u'_N}\,\ell Y_c + \left(\frac{3u''^{\,2}_N}{u'^{\,2}_N} - \frac{u'''_N}{u'_N}\right)\ell^2 Y_c^2 + O(\ell^3)\right], \\ &\tilde{g}(y) = 1 + \alpha_1(Y - Y_c) + \alpha_2(Y-Y_c)^2 + \cdots; \\ &\alpha_1 = -\frac{1-\mu}{2}\,\frac{N'_c}{N_c} + \frac{\ell u''_N}{2\mu u'_N}(1 + PN_c) + \frac{\ell^2}{2\mu}\left(\frac{u'''_N}{u'_N} - \frac{u''^{\,2}_N}{u'^{\,2}_N}\right) Y_c + \cdots, \\ &\alpha_2 = \frac{\mu\alpha_1^2}{1+2\mu} - \frac{PN''_c}{4(1+2\mu)} + \cdots. \end{aligned}\right\} \qquad (4.3)$$

The first of these equations, $\mu(1-\mu) = p$, has two roots

$$\mu = \mu_\pm = \tfrac{1}{2} \pm \sqrt{\tfrac{1}{4} - p}.$$

The solution of the problem (4.1) corresponding to the smaller of them will be referred to as the μ_- mode and the one corresponding to the greater as the μ_+ mode.

We encounter an unusual eigenvalue problem consisting of the second-order ordinary differential equation and three 'boundary conditions': Miles's condition (posed at the singular point) selects one of two linearly independent solutions of (4.1), and matching this solution to outer solutions $g_\pm(y)$ is achieved by choosing the parameters P and Y_c. In view of the proximity of y_c to y_N, we use for matching to the inner solution expansions of $g_\pm(y)$ calculated in the vicinity of $y = y_c$. They have a form which is standard for solutions of the Rayleigh equation (see, for example, Dikii 1976; Drazin & Reid 1981)

$$g_\pm(y) = a_\pm\left[1 + \frac{u''_c}{u'_c}\,(y-y_c)\ln|y-y_c| + \cdots\right] + b_\pm[(y-y_c) + \cdots]. \qquad (4.4)$$

Factors $a_\pm$ and $b_\pm$ depend on k and y_c, their ratios $(b/a)_\pm$ are real, and (for details, see Appendix A)

$$\left.\begin{array}{ll} 0 < b_-/a_- = O(1), \quad 0 < b_+/a_+ = O(k^{-1}) \gg 1 & \text{if } k \ll 1, \\ (b/a)_\pm = O(1) & \text{if } k = O(1), \\ -(b_+/a_+) \approx b_-/a_- \approx k \gg 1 & \text{if } k \gg 1. \end{array}\right\} \tag{4.5}$$

Let us divide our problem into two. First, for given $Y_c = Y_0$, we find solutions (eigenfunctions) of (4.1) satisfying Miles's condition (4.2) and the left (as $Y \to -\infty$) boundary condition as well as corresponding eigenvalues $P(Y_0; k)$. Then, bypassing the singular point $Y = Y_0$ from below, we continue these solutions analytically on the ray $Y > Y_0$, calculate their asymptotic expansions

$$g(Y) = A + B\,(Y - Y_c) + \cdots = A + \ell^{-1} B\,(y - y_c) + \cdots \tag{4.6}$$

as $Y \to +\infty$ and, matching them to (4.4), find the dependence $k(Y_0)$ that, being considered together with $P(Y_0; k)$, provides the dispersion relation $P = P(k)$ at the stability boundary. In § 3, it has been shown that when $k \gg 1$, the critical level of a marginally stable oscillation is outside of the transitional layer ($y_c - y_N \gg \ell$). Hence, considering SIP as complementary to RIP, we can restrict ourselves to the case $k\ell \ll 1$.

We search for the solution of 'a spectral problem to the left of Y_0' in the form of expansion in ℓ:

$$g = g^{(0)}(Y) + \ell g^{(1)}(Y) + \cdots, \quad P = P^{(0)} + \ell P^{(1)} + \cdots (\mu = \mu^{(0)} + \ell\mu^{(1)} + \cdots). \tag{4.7}$$

At $O(1)$ in view of (4.4), we obtain:

$$\left.\begin{array}{l} \dfrac{\mathrm{d}^2 g^{(0)}}{\mathrm{d}Y^2} + \dfrac{P^{(0)} N(Y)}{(Y_0 - Y)^2}\, g^{(0)} = 0, \quad \lim\limits_{Y \to -\infty} \dfrac{\mathrm{d}g^{(0)}}{\mathrm{d}Y} = 0; \\ g^{(0)}(Y) = (Y_0 - Y)^\mu \left[1 - \dfrac{1-\mu}{2}\, \dfrac{N_0'}{N_0}\, (Y - Y_0) + O((Y - Y_0)^2)\right] (|Y_0 - Y| \ll 1), \\ \mu(1-\mu) = P^{(0)} N_0 \equiv P^{(0)} N(Y_0) \leqslant \tfrac{1}{4}, \end{array}\right\} \tag{4.8}$$

(when Y_0 is bypassed by the Landau rule, $g^{(0)}(Y)$ acquires the factor $\exp(-\mathrm{i}\pi\mu)$ for $Y < Y_0$, but it does not play an essential role and will be omitted as will be the superscript (0) for μ).

4.2. *The spectrum of the problem* (4.8)

As does (3.5), this problem concerns zero energy level in the potential well of a given form with depth regulated by the stratification parameter ($P^{(0)}$), but is more complicated because the potential is singular. Like (3.5), it has an obvious (trivial) solution

$$P_0^{(0)} = 0, \quad g_0^{(0)}(Y) \equiv 1 \quad (\mu = 0). \tag{4.9}$$

To search for other (non-zero) eigenvalues we change variables in (4.8),

$$Y_0 - Y = \xi^\alpha, \quad g = (Y_0 - Y)^\lambda\, z(\xi) \equiv \xi^{(\alpha-1)/2}\, z(\xi), \quad \alpha = (1 - 2\lambda)^{-1} > 1,$$

where λ is the least root of the equation $\lambda(1-\lambda) = p \equiv P^{(0)} N_0$. (We assume $p < 1/4$, and the case $p = 1/4$ ($\lambda = 1/2$) can be considered as a limiting one.) We obtain

$$\frac{\mathrm{d}^2 z}{\mathrm{d}\xi^2} + \frac{\lambda(1-\lambda)}{(1-2\lambda)^2 \xi^2} \left[\frac{N(Y_0 - \xi^\alpha)}{N_0} - 1\right] z = 0 \quad (|z(+\infty)| < \infty). \tag{4.10}$$

The Miles condition with proper normalization takes the form: as $\xi \to 0$

$$z(\xi) = 1 + O(\xi^{\alpha}) \quad \text{for the } \mu_{-} \text{ mode} \quad (\text{i.e. when} \quad \mu = \lambda),$$
$$z(\xi) = \xi[1 + O(\xi^{\alpha})] \quad \text{for the } \mu_{+} \text{ mode} \quad (\text{i.e. when} \quad \mu = 1 - \lambda).$$

Continuing the potential in (4.10) onto $\xi < 0$ in such a way that it would be even, and adding the condition $|z| < \infty$ as $\xi \to -\infty$, we come to a new spectral problem, whose even solutions correspond to the μ_{-} mode whereas its odd solutions correspond to the μ_{+} mode. Clearly, non-trivial solutions ($\lambda > 0$) exist only when there is a potential well, i.e. a region in ξ where $N > N(Y_0)$. As $N(Y)$ has a single maximum ($N = N_M$ at $Y = Y_M$), such a well exists only if this maximum is situated to the left of Y_0 (i.e. if $Y_M < Y_0$). It also implies that any non-trivial solution of (4.8) (without loss of generality it can be considered as positive when $Y > Y_0$) increases monotonically and infinitely to the right of Y_0 so that in its asymptotic expansion (4.6) $B > 0$.

In Appendix C, it is shown that the problem (4.8) has at least one non-trivial solution for any $Y_0 > Y_M$ or, more precisely, an odd number of such solutions. If Y_0 is close enough to Y_M, the well in (4.10) is shallow and there is indeed only one solution. On the other hand, as $Y_0 \gg 1$, the spectrum of SIP should pass into the spectrum of RIP, therefore the number of non-trivial solutions should increase with growing Y_0, and new solutions should appear in pairs. How this proceeds we can understand by using the WKB solution of (4.10) (or considering a model spectral problem which can be solved exactly, see Appendix D) which yields the dispersion equation (for details, see Appendix C)

$$\sqrt{\mu(1-\mu)}\, D(Y_0) = m + \mu, \quad D(Y_0) = \frac{1}{\pi\sqrt{N_0}} \int_0^{x_0} \frac{\mathrm{d}x}{x} \sqrt{N(Y_0 - x) - N_0}, \tag{4.11}$$

where x_0 is the second (regular) turning point: $N(Y_0 - x_0) = N_0$. For each value of $D(Y_0) > 0$ (i.e. $Y_0 > Y_M$), this equation has an even number of roots

$$\left.\begin{aligned} &\mu_m^{(\pm)} = \frac{1}{2(1+D^2)} \left[D^2 - 2m \pm D\sqrt{D^2 - 4m(m+1)}\right] \left(0 \leqslant m \leqslant \frac{\sqrt{1+D^2}-1}{2}\right), \\ &\text{or} \\ &\left(P_m^{(\pm)} N_0\right)^{1/2} = \frac{1}{2(1+D^2)} [(2m+1)D \pm \sqrt{D^2 - 4m(m+1)}], \end{aligned}\right\} \tag{4.12}$$

including the root $\mu_0^{(-)} = 0$ ($P_0^{(-)} = 0$) which corresponds to the trivial solution (4.9), and this number increases with growing $D(Y_0)$. Namely, the mth pair of roots arises when $D = D_m = \sqrt{4m(m+1)}$ and exists as long as $D \geqslant D_m$, and in their origin both solutions belong to the μ_{-} mode because $\mu_m^{(\pm)}(D_m) = m/(2m+1) < 1/2$. With growing $D(Y_0)$, one root, monotonically decreasing, moves along a descending branch $\mu_m^{(-)}$ of the mth dispersion curve, and the other, monotonically increasing, moves along its ascending branch $\mu_m^{(+)}$, tending to 1. Transition of the solution from the μ_{-} to the μ_{+} mode (at $\mu_m^{(+)} = 1/2$) occurs when $D^2 = D_m^2 + 1 = (2m+1)^2$. Figure 3(*a*) shows results of numerical calculations of $P_m(Y_0)$ for model $N(Y)$ profile (2.5) and, for comparison, results of calculations in the WKB approximation for $m \geqslant 1$. Bold dots correspond to $\mu = 1/2$ and separate μ_{-} and μ_{+} modes.

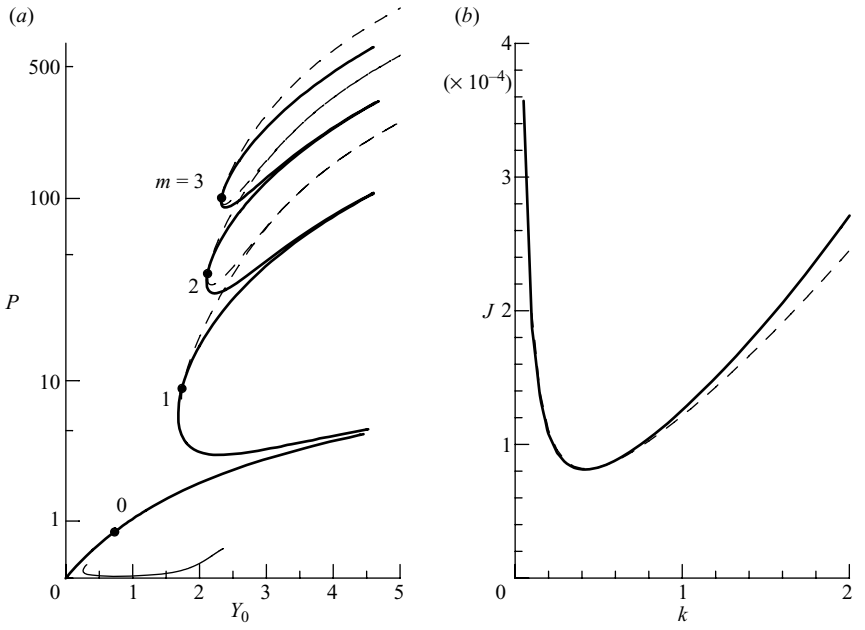

FIGURE 3. (*a*) Eigenvalues $P_m^{(0)}(Y_0)$ of the problem (4.8) (bold solid lines). WKB results are shown by dashes, and the lower branch of the $m = 0$ dispersion curve corrected for the finiteness of ℓ is shown by thin solid line. (*b*) Lower boundary of the instability domain ($m = 0$) calculated by numerically solving (2.3) (solid line) and by means of asymptotic formulae (4.14) and (4.17) (dashes).

For comparison with the spectrum of RIP we consider a limiting case $Y_0 \gg 1$. In this limit, the integral

$$D(Y_0) = \frac{1}{\pi\sqrt{N_0}} \int_{Y_0 - x_0}^{Y_0} \frac{\mathrm{d}Y}{Y_0 - Y} \sqrt{N(Y) - N_0} = \frac{1}{\pi Y_0 \sqrt{N_0}} \left[\int_{-\infty}^{\infty} \mathrm{d}Y \sqrt{N(Y)} + O\left(Y_0^{-1}\right) \right]$$

grows rapidly (at least, exponentially) with Y_0, and the number of eigenvalues of the problem (4.8) grows proportionally to it. As $D \gg m + 1$, it is found from (4.12) that

$$\mu_m^{(-)} = \frac{m^2}{D^2} + O\left[\left(\frac{m+1}{D}\right)^4\right], \quad \mu_m^{(+)} = 1 - \frac{(m+1)^2}{D^2} + O\left[\left(\frac{m+1}{D}\right)^4\right].$$

Because $P_m N_0 = \mu(1 - \mu)$,

$$P_m^{(\pm)} \approx \frac{\pi^2 (m+1)^2}{\left[\int_{-\infty}^{\infty} \mathrm{d}Y \sqrt{N(Y)}\right]^2} Y_0^2, \quad \text{for mode } \mu_+, \tag{4.13a}$$

$$P_m^{(\pm)} \approx \frac{\pi^2 m^2}{\left[\int_{-\infty}^{\infty} \mathrm{d}Y \sqrt{N(Y)}\right]^2} Y_0^2, \quad \text{for mode } \mu_-. \tag{4.13b}$$

Taking into account relationships between parameters P, R and J (see (3.3)), we see that when $1 \ll Y_0 \ll \ell^{-1}$, eigenvalues (4.13) of SIP are in satisfactory agreement with

eigenvalues of RIP (compare with (3.8) and (3.15)) if $m \geqslant 1$. At $m = 0$, WKB gives too rough an approximation and this case should be considered separately (see below).

The problem (4.8) and its solutions are the first approximation to solutions of (4.1). Calculation of the higher terms of the expansion (4.7) yields only small ($O(\ell)$) corrections to the spectrum already found. The branch $\mu_0^{(-)}$ described by the trivial solution (4.9) as well as the part of the branch $\mu_0^{(+)}$ corresponding to $Y_0 - Y_M = O(\ell)$ are obvious exceptions because for them 'corrections' are just the eigenvalues. Let us calculate the next term of expansion (4.7) after (4.9). From (4.1) at $O(\ell)$, we have:

$$\frac{\mathrm{d}^2 g_0^{(1)}}{\mathrm{d}Y^2} = \frac{u_N''}{u_N'(Y - Y_0)} - \frac{P_0^{(1)} N(Y)}{(Y - Y_0)^2},$$

$$g_0^{(1)} = \frac{u_N''}{u_N'}(Y - Y_0)[\ln \ell(Y - Y_0) - 1] - P_0^{(1)} \int_Y^\infty \frac{\mathrm{d}Y_1 N(Y_1)}{(Y_1 - Y_0)^2}(Y_1 - Y) + B_1(Y - Y_0).$$

Calculating asymptotic expansions of $g_0^{(1)}$ as $Y \to \pm\infty$ and matching $g_0 = 1 + \ell g_0^{(1)} + O(\ell^2)$ to (4.4), we obtain: $a_+ = 1$, $a_- = 1 + O(\ell)$, $B_1 = b_+ + O(\ell)$, and

$$P_0^{(1)} \int_{-\infty}^{\infty} \frac{\mathrm{d}Y N(Y)}{(Y - Y_0)^2} = b_- - b_+ + \mathrm{i}\pi \frac{u_c''}{u_c'} + O(\ell), \tag{4.14}$$

where $Y = Y_0$ is bypassed from below, and $b_\pm$ are real. The right-hand side of (4.14) depends on k through $(b_- - b_+)$ (see (4.5)), and since $u_c''/u_c' < 0$, its argument is between $-\pi$ and 0.

The imaginary part of the integral at the left-hand side is obviously equal to $\pi N_0'$. Because $N(Y)$ has a single maximum (at $Y = Y_M$), the real part of the integral is positive when $|Y_0| \gg 1$ and negative at $Y_0 = Y_M$, hence, its argument varies from 0 to $-\pi$ as Y_0 decreases from $+\infty$ to Y_M, and is subjected to further variation from $-\pi$ down to -2π as Y_0 decreases from Y_M to $-\infty$. The position $Y_0(k)$ of the critical level of marginally stable perturbation is obviously such that arguments of the right- and left-hand sides of (4.14) are equal. Hence, when stratification is stable ($P > 0$), $Y_0 > Y_M$ on the stability boundary.

In the framework of RIP, $J_0^{(-)}(k)$ was found for $k \gg 1$ and $k < \ell \ll 1$. Let us see what (4.14) yields in these cases. When $k \gg 1$, $b_- - b_+ \approx 2k$ (see (4.5)) and

$$\frac{J}{\ell^2 {u_c'}^2}\left(\text{f.p.} \int_{-\infty}^{\infty} \frac{\mathrm{d}Y N(Y)}{(Y - Y_0)^2}\right) \approx 2k, \quad \frac{J N_0'}{\ell^2 {u_c'}^2} = \frac{u_c''}{u_c'},$$

where f.p. stands for the finite (or, which is the same in this case, real) part of the integral. The right-hand side of (4.14) has a small ($O(k^{-1})$ negative argument, hence $Y_0 \gg 1$ and

$$\frac{J N_0'}{\ell^2 {u_c'}^2} = \frac{u_c''}{u_c'}, \quad \frac{J}{\ell^2 {u_c'}^2 Y_0^2} \approx 2k, \tag{4.15}$$

which coincides with relations (3.23) and (3.24) describing the lower boundary in the framework of RIP. In an opposite limit, $k \ll 1$, $0 < b_+ - b_- \approx {u_c'}^2/[k(1-c)^2]$ (see (4.5) and (A11)). Hence, the argument of the right-hand side of (4.15) is close to $-\pi$, $Y_0 = Y_M + O(k)$ and

$$P_0^{(1)} N_0' = \frac{u_c''}{u_c'}, \quad P_0^{(1)} \approx \frac{{u_c'}^2}{k(1-c)^2}\left(\int_{-\infty}^{\infty} \frac{\mathrm{d}Y}{(Y - Y_M)^2}[N_M - N(Y)]\right)^{-1}. \tag{4.16}$$

In the next ($O(\ell^2)$) order, we also obtain the complex-valued equation

$$\left(\frac{P_0^{(2)}}{P_0^{(1)}} - \frac{2u_N'' Y_0}{u_N'}\right)\int_{-\infty}^{\infty}\frac{\mathrm{d}Y N(Y)}{(Y-Y_0)^2} + 2(\delta Y_0)\int_{-\infty}^{\infty}\frac{\mathrm{d}Y N(Y)}{(Y-Y_0)^3}$$
$$= \left[\frac{u_N''}{u_N'}(3-2\ln\ell) - \frac{2G_c'}{G_c}\right]\int_{-\infty}^{\infty}\frac{\mathrm{d}Y N(Y)}{Y-Y_0} - \frac{2u_N''}{u_N'}\int_{-\infty}^{\infty}\frac{\mathrm{d}Y N(Y)}{Y-Y_0}\ln(Y-Y_0)$$
$$-2P_0^{(1)}\int_{-\infty}^{\infty}\frac{\mathrm{d}Y N(Y)}{Y-Y_0}\int_{Y}^{\infty}\frac{\mathrm{d}Y_1 N(Y_1)}{(Y_1-Y_0)^2}, \tag{4.17}$$

that allows us to calculate (real) corrections to the eigenvalue ($P_0^{(2)}$) and to the position of the critical level (δY_0), etc. The resulting dependence $P_0(Y_0) = \ell P_0^{(1)} + \ell^2 P_0^{(2)} + O(\ell^3)$ describes the branch $\mu_0^{(-)}$ corrected for the finiteness of ℓ. This solution is valid when $|\ell P_0^{(1)}| \ll 1$, or, as follows from (4.16), when $k \gg \ell$, i.e. far from the region $k < \ell$ where RIP works. Continuation of (4.16) into smaller k is associated, as we shall see further, with motion along the branch $\mu_0^{(+)}$. The corrected $\mu_0^{(-)}$ branch is shown in figure 3(a) (by thin line) and, in the form $J = J_0^{(-)}(k)$, in figure 3(b). In figure 3(a), we can see how this branch will connect with the (corrected as well) branch $\mu_0^{(+)}$ to give a corrected $P = P_0(Y_0)$ curve. It is evident that this curve will run to neither $Y_0 = Y_M$ nor $P = 0$. (It is shown in Appendix C that the $P = P_0(Y_0)$ curve is rounded when P and $(Y_0 - Y_M)$ are both of $O(\ell^{1/2})$.)

Note that, according to (4.15) and (4.16), the resulting dependence $J = J_0^{(-)}(k)$ is a function decreasing when $k \ll 1$ and growing when $k \gg 1$, i.e. having a minimum at $k = O(1)$. In this case, the module and the argument of the right-hand side of (4.14) are both of the order of unity, so that $Y_0 = O(1)$, $P_{0\,min}^{(1)} = O(1)$ and

$$J_* = \min_k J_0^{(-)}(k) = \ell {u_N'}^2 P_{0\,min} \approx \ell^2 {u_N'}^2 P_{0\,min}^{(1)} = O(\ell^2),$$

in complete agreement with an estimate (3.25). Exact values of J_* and of corresponding k depend, obviously, on profiles of velocity and density and can be found only numerically.

4.3. *Spectrum of SIP, matching to RIP and lower boundaries of instability domains*

Thus, we have shown that SIP has eigenvalues only when $Y_0 > Y_M$, their number is even and grows proportionally to $D(Y_0)$. When $1 \ll Y_0 \ll \ell^{-1}$, the domains of validity of RIP and SIP overlap and their spectra are in reasonable agreement (compare (3.8) and (3.21) with (4.13)) but a 'splitting' takes place: two eigenvalues of SIP, $P_m^{(\pm)}$, correspond to the eigenvalue R_m of RIP with the same m, with one eigenvalue of SIP belonging to the μ_+ mode and the other to the μ_- mode. On the other hand, RIP can describe the lower boundaries of particular instability domains only in two extreme bands of k, when either $0 \leqslant k < \ell \ll 1$ or $k \gg 1$. It is reasonable to suppose that solutions of RIP match the μ_+ mode on one of these extremities and the μ_- mode on the other.

Indeed, for any m, it can be shown (for details, see Appendix C) that on the long-wavelength ($k < \ell$) end of the oscillation spectrum, as the critical level 'intrudes' (with increase in k) into a peripheral region ($1 \ll Y_0 \ll \ell^{-1}$) of the transitional layer, the solution of RIP passes into the μ_+ mode of SIP with $\mu \approx 1$. Further, as we moves along the dispersion curve $P = P_m(Y_0)$ (or, otherwise, $P = P_m(\mu)$) corrected for the finiteness of ℓ towards a decrease of μ (first along the branch $\mu_m^{(+)}$ and then along

the branch $\mu_m^{(-)}$), k grows, and the μ_- mode of SIP (with μ close to zero) should pass ultimately into solution of RIP.

This scenario is fulfilled very well at $m=0$. It can be shown (see Appendix C) that transition between $\mu_0^{(+)}$ and $\mu_0^{(-)}$ branches takes place when k, P_0 and Y_0 are all of $O(\ell^{1/2})$. As we have seen earlier, the μ_- mode describes the lower stability boundary from this point up to $1 \ll k \ll \ell^{-1}$ where a smooth transition takes place to the boundary calculated within the RIP. However, if $m>0$ the passage from $k=O(\ell)$ to $k=O(1)$ is not so straightforward.

To understand the difficulty here we consider the second part of SIP, namely, we continue (using the Landau rule) each of the found eigenfunctions of (4.8) on the ray $Y>Y_0$, then, having calculated the ratio of the coefficients A and B of its asymptotic (as $Y-Y_0 \gg 1$) expansion (4.6), we match this continued eigenfunction to the outer solution $g_+(y)$ and thereby find $k=k_m(\mu)$. These relations, together with eigenvalues $P=P_m(\mu)$ of (4.8), set lower boundaries $J=J_m^{(-)}(k)$ in a parametric form. As was mentioned earlier, $B>0$, hence, $B/A=O(1)$ or even greater (see Appendix C), and for matching to (4.4) b_+/a_+ must be $O(\ell^{-1})$ or greater. In accordance with (4.5) this corresponds to $k=O(\ell)$.

However, it does not mean that within the framework of SIP it is impossible to describe perturbations with $k>\ell$. The difficulty is that the problem (4.8), as the first approximation to SIP, is not an approximation uniformly valid for all Y_0. Namely, it yields correct asymptotics (4.6) of eigenfunctions when $\mu \gg \ell$, but its results are incorrect when $\mu=O(\ell)$ or less.

To verify this, suppose that 'the spectral problem to the left of Y_0' is solved, and the spectrum of SIP $P=P_m(Y_0)$ is known. Let us choose some $m \geqslant 1$ and examine more attentively SIP and its solutions when $Y>Y_0>Y_M$ and $\mu=\mu_- \approx PN_0 \ll 1$. Since $N(Y)$ decreases rapidly (exponentially), μ becomes of the same order as ℓ already for not so great values of Y_0, namely, for $Y_0=O(\ln \ell^{-1})$ or even less, and this fact implies two significant consequences for solutions of SIP. First, the second term in the coefficient α_1 of the Miles expansion (see (4.2) and (4.3)) increases up to $O(1)$ and starts to compete with the first term so that

$$g(Y)=1-\frac{1}{2}\left(\frac{N_0'}{N_0}-\frac{\ell u_N''}{PN_0u_N'}\right)(Y-Y_0)+O(PN_0+\ell) \quad (0<Y-Y_0 \ll 1). \tag{4.18}$$

Secondly, in (4.1) the first term in braces (and, together with it, the entire expression in them) becomes $O(\ell)$. Hence, when $Y>Y_0$, the solution of (4.1) can be written as $g(Y)=A+B(Y-Y_0)+O(\ell)$, and matching it to (4.18) yields

$$A=1+O(PN_0+\ell), \quad B=\frac{1}{2}\left(\frac{\ell u_N''}{PN_0u_N'}-\frac{N_0'}{N_0}\right)+O(PN_0+\ell).$$

As a result, unlike the problem (4.8), the factor B is no longer positive for all Y_0. It is positive when $Y_0<Y_*$, equal to zero at $Y_0=Y_*$ (Y_* depends on m (as $P_m(Y_0)$ does), namely, it slowly (logarithmically) increases with m), where (compare with (3.23) and the first relation in (4.16))

$$PN_0'=\frac{\ell u_N''}{u_N'}+O(\ell^2), \tag{4.19}$$

and negative when $Y_0>Y_*$ (recall that $N_0'<0$ and $u_N''<0$). This opens for SIP a way from $k=O(\ell)$ not only to $k=O(1)$ but also into domain $k \gg 1$ where A and B should have opposite signs (see (4.5)).

It is necessary now to specify a procedure for finding eigenvalues $P = P_m(Y_0)$ of SIP which would take into account reordering in Miles's condition when $\mu = O(\ell)$. The solution of (4.1) for $Y < Y_c$ is constructed as before, in the form of expansion in ℓ:

$$g = g^{(0)} + \ell g^{(1)} + \cdots, \quad P = P^{(0)} + \ell P^{(1)} + \cdots, \quad Y_c = Y_0 + \ell Y_1 + \cdots, \tag{4.20}$$

In this case, the function $g^{(0)}$, at $O(1)$, obeys the same equation and left (as $Y \to -\infty$) boundary condition (4.8), but the boundary condition at $Y \to Y_0$ is to be changed. Because its essential change is required only when $\mu = O(\ell)$, for the μ_+ mode (i.e. for $\mu \geqslant 1/2$) we retain the old boundary condition,

$$\left.\begin{aligned} &g^{(0)}(x) = x^{\mu^{(0)}} H\big(x;\mu^{(0)}\big), \quad x = Y_0 - Y, \quad \mu^{(0)}\big(1-\mu^{(0)}\big) = P^{(0)} N_0, \\ &H(x;\mu) = 1 + \frac{1-\mu}{2}\,\frac{N_0'}{N_0}\,x + O(x^2), \end{aligned}\right\} \tag{4.21}$$

and for the μ_- mode ($0 < \mu \leqslant 1/2$) we take it in a modified form

$$g^{(0)}(x) = x^{\mu^{(0)}} H\big(x;\mu^{(0)}\big) - T x^{1-\mu^{(0)}} H\big(x;1-\mu^{(0)}\big), \quad T = \frac{\ell u_N''}{2\mu^{(0)} u_N'}. \tag{4.22}$$

It is easy to see that at $\mu^{(0)} = 1/2$, boundary conditions (4.21) and (4.22) are in essence identical, hence the $P^{(0)}(Y_0)$ dependence remains continuous. As long as $\mu^{(0)} \gg \ell$, the term with a 'foreign' degree of x due to (4.22) is small and when matching to Miles's expansion (see (4.2) and (4.3)) is compensated by contributions from the higher orders of the expansion (4.20) while $P^{(0)}(Y_0)$ has an addition of $O(\ell/\mu^{(0)})$. In substance, we obtain in this case only a somewhat different (as compared to the one found earlier) way for expanding the same $P(Y_0)$ in ℓ. When, however, $\mu^{(0)} = O(\ell)$, the terms in the right-hand side of the boundary condition (4.22) become of the same order and, as shown in Appendix E, this choice of the factor T allows us to fit the expansion (4.20) to the re-ordering in the Miles condition. The procedure of calculating the eigenvalues and eigenfunctions is detailed in Appendix E. The corrected dependences of $P_m^{(0)}$ on Y_0 and of B/A on μ are shown in figure 4.

Let us draw our attention to the difference in B/A behaviour at $m = 0$ and $m > 0$ (see figure 4*b*). According to (4.5), when B/A rises from -1 to $+1$, k runs from $O(\ell^{-1})$ to $O(\ell)$, i.e. through the entire 'responsibility band' of SIP. As $m \geqslant 1$, this change in B/A takes place in a fairly narrow range of μ (and Y_0) where $|T| = O(1)$, namely, in the vicinity of points marked by triangles in figure 4(*a*). For this reason $J = J_m^{(-)}(k)$, after attaining its minimal value, grows very slowly with k (see figure 2*b*). On the contrary, if $m = 0$, B/A remains near zero when μ (as well as T, see (4.22)) changes by a factor of about 300. The reason is that the condition (4.19) for $B = 0$ is almost the same as the imaginary part of the dispersion equation (4.14) of the mode $m = 0$ and holds approximately in a wide range of Y_0.

Lastly, in figure 5 we plot eigenfunctions $g_m(Y)$ of marginally stable oscillations with $k = k_* \approx 0.4159$ (where $J_0^{(-)}(k)$ attains its minimum) and $m = 0$, 1, 2, 3. (more precisely, they are $g_m(Y)$ if $Y < Y_c$, and $|g_m(Y)| = g_m(Y)\exp(-\mathrm{i}\pi\mu)$ if $Y > Y_c$). The mth eigenfunction has m nodes and a branch point at $Y = Y_c$ (see (4.2)) with a very small $\mu = O(\ell)$. Note that all nodes are located below the critical level, in a good agrement with instability interpretation in terms of overreflection (see, for example, Davis & Peltier 1976, 1979; Smyth & Peltier 1989).

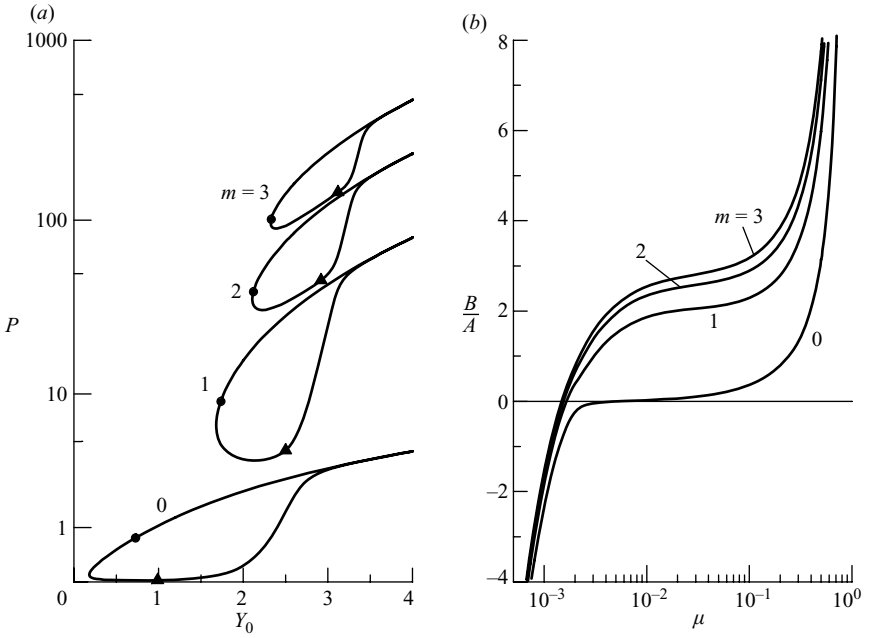

FIGURE 4. (*a*) Eigenvalues $P_m^{(0)}(Y_0)$ of SIP, and (*b*) the μ dependence of the B/A ratio under boundary condition (4.22). Bold dots correspond to $\mu^{(0)} = 1/2$ and separate μ_- and μ_+ modes, triangles mark points where $|T| = 1$.

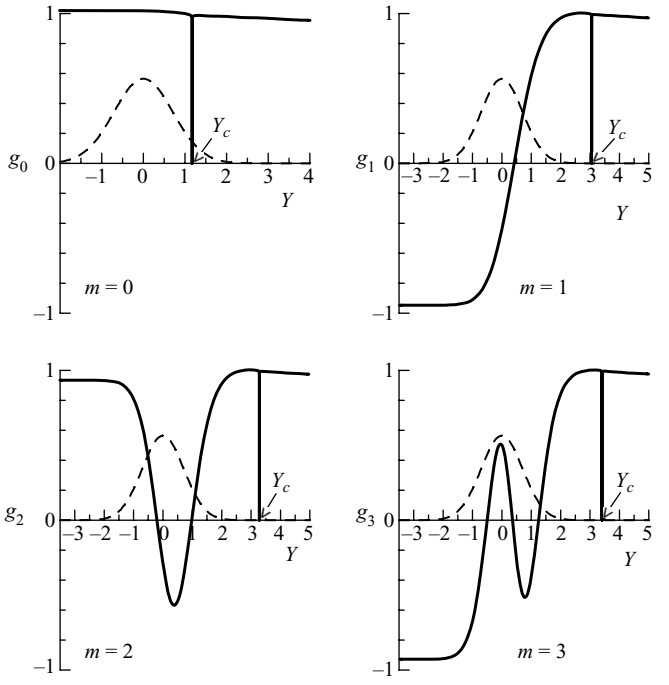

FIGURE 5. Eigenfunctions $g_m(Y)$ of marginally stable oscillations. For reference, $N(Y)$ profile is shown by dashes.

5. Discussion of results

Thus, we have found the spectrum of eigenoscillations and the configuration of the instability domain for a wide enough class of shear flows of ideal fluid, namely, for flows with a bounded monotonically increasing inflection-free velocity profile ($0 \leqslant u(y) < U_0 = 1,\ u'(y) > 0,\ u''(y) < 0$) and with density continuously stratified in a layer centred at $y = y_N$ and having the width ℓ much less than the scale of velocity variation $L = 1$. (We represent the squared buoyancy frequency in the form $\Omega^2(y) = J\, n(y)$ so as to describe its 'profile' and 'magnitude' by normalized (see (2.1)) function $n(y)$ and the bulk Richardson number J, respectively.) Let us discuss and compare them with the spectrum of oscillations and configuration of the instability domain of two-layer flows ($\ell = 0$).

Both for $\ell = 0$ and for $\ell \neq 0$, the spectrum contains 'fast' (propagating with phase velocity $c \geqslant 1$) neutral oscillations and 'slow' unstable oscillations (their velocities are in the range $u_N \equiv u(y_N) < c_r < 1$). When $\ell = 0$, both kinds of oscillation are conveniently displayed on the $(k,\ J)$-diagram where they occupy, respectively, regions above and below the curve $J = J_1(k)$ which is, at the same time, the dispersion curve of neutral oscillations with $c = 1$ and the upper boundary of the instability domain (see figure 1). When $\ell \neq 0$, the nodeless ($m = 0$) mode also exists and has a very similar $(k,\ J)$-diagram. Moreover, its own $(k,\ J)$-diagram corresponds to each $m = 1,\ 2,\ 3\ldots$ (see figure 2*b*) so that the complete stability diagram of the flow consists of a denumerable set of $(k,\ J)$ sheets. On each of them, fast (neutral) and slow (unstable) oscillations are separated by the dispersion curve $J = J_m(k; 1)$ of the corresponding (mth) branch of neutral oscillations with $c = 1$ (see figure 2*a*). It is interesting to note that a similar structure of the spectrum of Holmboe's waves was obtained by Alexakis (2005) for (inflected) $u = \tanh y$ and $n = (R/2)\mathrm{sech}^2(Ry)$ when $R > 2$.

Another crucial difference is that when $\ell \neq 0$, there appear lower boundaries of instability domains, $J = J_m^{(-)}(k) > 0$, whose position is the higher, the greater m. At $k = 0$, the lower boundary joins the upper one ($J_m^{(-)}(0) = J_m(0; 1)$). As k grows, it falls abruptly (almost vertically) downwards, reaches its minimum ($J = J_* = O(\ell^2)$ at $k = k_0 = O(1)$ if $m = 0$, and $J = O(m^2\ell)$ at $k = k_m = O(\ell/m)$ if $m \geqslant 1$), and then starts to rise slowly (see figure 2*b*). Such behaviour of $J_m^{(-)}(k)$ becomes clear if we take into account the fact that of the two mechanisms responsible for instability of shear flows, the resonance and non-resonance mechanisms (see, for example, Churilov & Shukhman 2001), it is the resonance mechanism that plays the governing role in the vicinity of the stability boundary. It is based on the resonance interaction of a perturbation wave with the flow in the critical layer (surrounding the critical level $y = y_c$), resulting in the perturbation, on the one hand, being amplified owing to the velocity shear (because $u''(y) < 0$, see, for example, Fabrikant 2002; Timofeev 2000), while, on the other, being absorbed, owing to stable stratification. The exact balance of these processes is achieved just on the stability boundary (see (3.18) and (3.23)).

Recall that the stratification which is responsible for absorption of oscillations is located in a narrow transitional layer and rapidly decays outside of it. For this reason, in a very wide wavelength range ($\ell < k < \ell^{-1}$), the critical level of marginally stable oscillations is forced to be located either inside of the transitional layer or on its near periphery ($y_c - y_N \ll 1$), and this explains the slow variation of $J_m^{(-)}$ with k, as well as its smallness in comparison with values of $J = J_m(k; 1)$ on the upper boundary of the same (mth) instability domain (see (3.3)). It is only when the amplification factor reduces in the long-wavelength range (see (3.17)) that the critical layer (i.e. the region of resonance wave–flow interaction) is able to leave the vicinity of the transitional layer and to move toward the flow periphery, as is readily seen in a model example

(see (3.19) and (3.20)). As a result, when $k \to 0$, velocity c increases, tending to 1, and $J_m^{(-)}$ sharply increases, and at $k = 0$, the lower boundary of the instability domain joins the upper one.

As can be seen in figure 2 (*b*), all sheets of the new stability diagram are arranged in the same manner. Roughly speaking, the sheet with number $m \geqslant 1$ can be made from the zeroth one ($m = 0$) by contracting it m/ℓ times in k and stretching m^2/ℓ times in J. Comparison of the zeroth sheet with the (k, J)-diagram for two-layer flow (see figure 1) shows that the fundamental (and practically unique) distinction between them consists in a strip of stability ($0 < J \leqslant J_0^{(-)}(k)$) appearing in continuously stratified flows when the density difference across the flow is small. There are similar (but much wider) strips on the other sheets, too.

Bringing together all the particular instability domains, we obtain the total instability domain of the flow. In the combined (k, J)-diagram (constructed by superimposing all sheets) it is bounded from below by the curve $J = J_0^{(-)}(k)$, but has no upper boundary. Outside of the total instability domain, there remain only the strip of stability $0 < J \leqslant J_0^{(-)}(k)$ in the lower part of the diagram and a chain of small triangular 'stability islands' extended along the J-axis: the mth island is limited by the ordinate axis ($k = 0$), the mth upper ($J = J_m(k; 1)$) and the ($m + 1$)th lower ($J = J_{m+1}^{(-)}(k)$) boundaries of the particular instability domains. Note that for each $J > J_*$ the total instability domain now has a finite width in k, $k_-(J) < k < k_+(J)$.

Particular instability domains on the combined (k, J)-plane mutually overlap and at given J, several oscillations may prove to be unstable which have the same k, but different m and various growth rates. In § 3, we have established that oscillations with $m = 0$ have a maximum growth rate $\gamma_0 = O(1)$ whereas when $m \geqslant 1$ it is markedly less, $\gamma_m = O(\ell/m)$. On the other hand, numerical calculations for model flow (2.5) show that for fixed m and k, the growth rate reaches a maximum when J is close to the mth lower boundary, and decreases rather rapidly both downwards and upwards. Therefore, at given J, among unstable oscillations with the same k, the maximum growth rate does not necessarily belong to the oscillation with smaller m (even if $m = 0$).

During this study, it was assumed everywhere that the medium is an ideal fluid, and only two-dimensional (independent of the z-coordinate) perturbations were considered. Abandoning these restrictions changes the above picture noticeably. Thus, for example, if we take into account, even weak, dissipation, the instability domain of the flow turns out to be markedly reduced, first of all, because only a finite number obviously remains of the denumerable set of particular instability domains. On the mth sheet, the maximum growth rate and characteristic vertical scale of variation of eigenfunctions have the same order, $\gamma_m \sim l_m = O(\ell/m)$, hence, the minimum $m = m_*$, at which all unstable oscillations are already suppressed by dissipation, and, because of that, the upper boundary of the total instability domain can be estimated as

$$m_* = O\left(\ell/\nu^{1/3}\right), \quad J_{tot}^{(+)} \sim J_{m_*}^{(-)} = O(m^2\ell) = O\left(\ell^3/\nu^{2/3}\right),$$

where ν is a (dimensionless) characteristic diffusivity (of momentum, heat, salt, etc.). By analogy, we may conclude that the instability domain should be bounded by dissipation from the short-wavelength side, as well.

Conversely, giving up the two-dimensionality of perturbations results in an expanded instability domain and, which is more essential, in crucial changes to its configuration. As Squire (1933) has established, the flow stability with respect to three-dimensional (oblique) perturbations is related to that with respect to two-dimensional disturbances. In our case (stratified flows described in the Boussinesq

approximation), this relation is as follows (for more detail see Smyth, Klaassen & Peltier 1989; Smyth & Peltier 1990): the problem of evolution (with time t) of three-dimensional perturbations with the wave vector $\boldsymbol{k}_3 = (k\cos\phi,\ 0,\ k\sin\phi)$ in the flow with $V_x = u(y)$ and $n = n(y)$ (see § 2) is reduced, using the transformation

$$t' = \eta t, \quad Re' = \eta Re, \quad J' = \eta^{-2} J, \quad Pr' = Pr; \quad \eta = \cos\phi, \tag{5.1}$$

to a problem of evolution (with time t') of two-dimensional perturbations with the wave vector $\boldsymbol{k}_2 = (k,\ 0,\ 0)$ in the flow with the same $V_x = u(y)$, $n = n(y)$ and Prandtl number Pr, but Reynolds and bulk Richardson numbers modified in accordance with (5.1), i.e. $Re \to Re'$ and $J \to J'$. In particular, the growth rates of three- and two-dimensional perturbations are related by

$$\gamma(k,\ \phi; J, Re, Pr) = \eta\,\gamma(k,\ 0; \eta^{-2} J, \eta Re, Pr), \tag{5.2}$$

and this relation dictates the character of changes in the instability domain configuration when we switch from two-dimensional to oblique perturbations.

According to (5.2), in the case of ideal fluid flows ($Re = \infty$) the mth sheet of the $(k,\ J)$-diagram for oblique perturbations with given ϕ can be made from the mth 'two-dimensional' sheet by contracting it η^{-2} times in J so that the upper and lower boundaries of the mth instability domain are η^{-2} times lower than at $\phi = 0$. In particular, the lower boundary of the total instability domain, $J = J_0^{(-)}(k;\phi) \equiv J_0^{(-)}(k)\cos^2\phi$, runs lower than in the case of two-dimensional perturbations. Hence, in the class of flows under consideration, three-dimensional perturbations are the first to lose stability when stratification reinforces, whereas two-dimensional perturbations require greater values of the bulk Richardson number in order to grow. Considering oblique perturbations with all possible ϕ, we can now conclude that for any $k > 0$ and $J > 0$, there is at least one unstable oscillation, i.e. that the instability domain begins immediately above the abscissa axis (as if $\ell = 0$, see figure 1) and occupies all the $(k,\ J)$-diagram.

Figure 6 demonstrates (for the flow (2.5)) the ϕ-dependence of the perturbation growth rate for $k = k_*$ (where $J_0^{(-)}(k)$ attains its minimum) and various values of J as well as competition between modes with different m. Since instability thresholds for two-dimensional disturbances with $m = 0$ and $m > 0$ are highly different (see figure 2*b*), the nodeless mode is undoubtedly dominant when $J \ll 1$. If stratification is 'subcritical' ($J < J_*$, figure 6*a*) a 'cone of stability' exists because only perturbations with $\cos\phi < J/J_*$ are unstable. When $J > J_*$, the instability takes place for any ϕ, but as long as the 'supercriticality' is weak or moderate, oblique disturbances grow faster than two-dimensional ones (see figure 6*b*, *c*). Only if the stratification is so strong that $\mathrm{d}(\ln\gamma)/\mathrm{d}(\ln J) < 1/2$ at $\phi = 0$, do two-dimensional oscillations have a higher growth rate in comparison with oblique disturbances with the same m (figure 6*d*).

It should be mentioned, however, that, because the mth instability domain has (at $\phi = 0$) the upper boundary $J = J_m(k;1)$, disturbances with $\cos\phi \leqslant J/J_m(k;1)$ belonging to the mth mode are stable (as can be seen in figure 6*d*–*f*). Hence, as ϕ is close enough to $\pi/2$, the $(m+1)$th mode competes with the mth mode, the $(m+2)$th mode competes with the $(m+1)$th mode, and so on. As J approaches $J_m(k;1)$, the range of ϕ in which the $(m+1)$th mode grows faster than the mth mode becomes wider and wider and ultimately reaches $\phi = 0$ (see figure 6*e*, *f*; in the flow (2.5) $J_0(k_*;1) = 1.2205$). With J increasing further, the $(m+1)$th and $(m+2)$th modes begin to compete in a wide range of ϕ, and so on.

Therefore, we see that in flows of the class under consideration, the primary instability generates, as a rule, three- rather than two-dimensional disturbances and

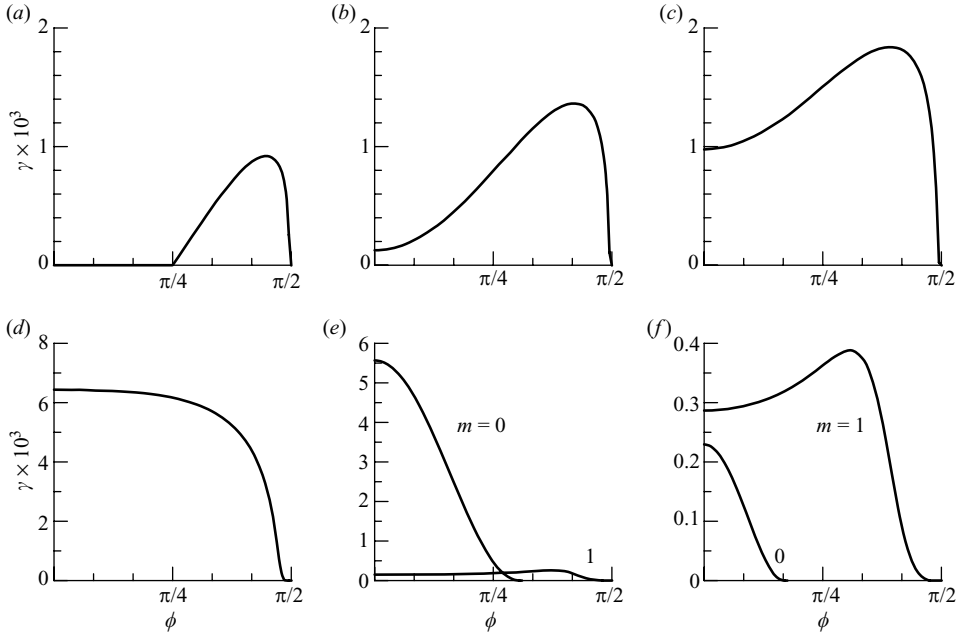

FIGURE 6. Plots of $\gamma \times 10^3$ *versus* ϕ for nodeless ($m = 0$) mode at (*a*) $J = J_*/2$, (*b*) $J = 1.1\,J_*$, (*c*) $J = 2\,J_*$ and (*d*) $J = 0.002\,(\approx 24\,J_*)$, and comparison of $m = 0$ and $m = 1$ modes at (*e*) $J = 0.4$ and (*f*) $J = 0.9$.

transition to turbulence does not require a two-dimensional stage and secondary instability. Note that the possibility for three-dimensional perturbations development due to primary instability of the stratified shear flow (of a mixing-layer type) has been demonstrated by Smyth & Peltier (1990), but only for moderate Reynolds numbers ($Re < 500$). In our case, it takes place at high Reynolds numbers, as well.

The author is grateful to Professor W. D. Smyth for helpful comments and criticism during the review process.

The work was supported in part by Programs of Russian Academy of Sciences Presidium no. 16 and OFN RAS no. 16, and by 'Leading Scientific Schools' Grants no. 7629.2006.2 and no. 900.2008.2 provided by the Ministry of Industry, Science and Technology of the Russian Federation.

REFERENCES

ABRAMOWITZ, M. & STEGUN, I. A. 1964 *Handbook of Mathematical Functions*. Natl Bureau of Standards.

ALEXAKIS, A. 2005 On Holmboe's instability for smooth shear and density profiles. *Phys. Fluids* **17**, 084103.

CALOGERO, F. 1967 *Variable Phase Approach to Potential Scattering*. Academic.

CHIMONAS, G. 1974 Considerations of the stability of certain heterogeneous shear flows including some inflexion-free profiles. *J. Fluid Mech.* **65**, 65–69.

CHURILOV, S. M. 2004 On the stability of stratified shear flows with a monotonic velocity profile without inflection points. *Izv. Atmos. Ocean. Phys.* **40**, 725–736.

CHURILOV, S. M. 2005 Stability analysis of stratified shear flows with a monotonic velocity profile without inflection points. *J. Fluid Mech.* **539**, 25–55.

Churilov, S. M. & Shukhman, I. G. 2001 Kinetic and hydrodynamic aspects of the instability of shear flows. *Izv. Atmos. Ocean. Phys.* **37**, 113–121.

Davis, P. A. & Peltier, W. R. 1976 Resonant parallel shear instability in the stably stratified planetary boundary layer. *J. Atmos. Sci.* **33**, 1287–1300.

Davis, P. A. & Peltier, W. R. 1979 Some characteristics of the Kelvin–Helmholtz and resonant overreflection modes of shear flow instability and of their interaction through vortex pairing. *J. Atmos. Sci.* **36**, 2394–2412.

Dikii, L. A. 1976 *Hydrodynamic Stability and Atmospheric Dynamics*. Gidrometeoizdat (in Russian).

Drazin, P. G. & Reid, W. H. 1981 *Hydrodynamic Stability*. Cambridge University Press.

Fabrikant, A. 2002 Plasma-hydrodynamic analogy for waves and vortices in shear flows. In *Sound-Flow Interactions* (ed. Y. Aurégan, A. Maurel, V. Pagneux & J.-F. Pinton). Lecture Notes in Physics, vol. 586, pp. 192–209. Springer.

Fedoryuk, M. V. 1983 *Asymptotic Methods for the Linear Ordinary Differential Equations*. Nauka (in Russian).

Fua, D., Einaudi, F. & Lalas, D. P. 1976 The stability analysis of an inflexion-free velocity profile and its application to the night-time boundary layer in the atmosphere. *Boundary-Layer Met.* **10**, 35–54.

Howard, L. N. 1961 Note on a paper by John W. Miles. *J. Fluid Mech.* **10**, 509–512.

Miles, J. W. 1961 On the stability of heterogeneous shear flows. *J. Fluid Mech.* **10**, 496–508.

Miles, J. W. 1963 On the stability of heterogeneous shear flows. Part 2. *J. Fluid Mech.* **16**, 209–227.

Nayfeh, A. H. 1973 *Perturbation Methods*. Wiley.

Olver, F. W. J. 1974 *Asymptotics and Special Functions*. Academic.

Redekopp, L. G. 2001 Elements of instability theory for environmental flows. In *Environmental Stratified Flows* (ed. R. Grimshaw), pp. 223–281. Kluwer.

Smyth, W. D. & Peltier, W. R. 1989 The transition between Kelvin–Helmholtz and Holmboe instability: an investigation of of the overreflection hypothesis. *J. Atmos. Sci.* **46**, 3698–3720.

Smyth, W. D. & Peltier, W. R. 1990 Three-dimensional primary instabilities of a stratified, dissipative, parallel flow. *Geophys. Astrophys. Fluid Dyn.* **52**, 249–261.

Smyth, W. D., Klaassen, G. P. & Peltier, W. R. 1989 Finite amplitude Holmboe waves. *Geophys. Astrophys. Fluid Dyn.* **43**, 181–222.

Squire, H. B. 1933 On the stability of three-dimensional disturbances of viscous flow between parallel walls. *Proc. R. Soc. Lond.* A **142**, 621–628.

Timofeev, A. V. 2000 *Resonance Phenomena in Oscillations of Plasma*. Fizmatlit (in Russian).

Turner, J. S. 1973 *Buoyancy Effects in Fluids*. Cambridge University Press.